MRS Advances © 2019 Materials Research Society
DOI: 10.1557/adv.2019.286

MRS Advances

Plasmonic Response of Light-Activated, Nano-Gold Doped Polymers

Jessica M. Andriolo,[1,2] McKenzie L. Joseph,[1,2] Molly C. Brockway,[2,3] and Jack L. Skinner[1,2,3]

[1]*Mechanical Engineering, Montana Technological University, Butte, MT 59701*

[2]*Montana Tech Nanotechnology Laboratory, Butte, MT 59701*

[3]*Materials Science Ph.D. Program, Montana Technological University, Butte, MT 59701*

Abstract

Incorporation of metallic nanoparticles (NPs) in polymer matrix has been used to enhance and control dissolution and release of drugs, for targeted drug delivery, as antimicrobial agents, localized heat sources, and for unique optoelectronic applications. Gold NPs in particular exhibit a plasmonic response that has been utilized for photothermal energy conversion. Because plasmonic nanoparticles typically exhibit a plasmon resonance frequency similar to the visible light spectrum, they present as good candidates for direct photothermal conversion with enhanced solar thermal efficiency in these wavelengths. In our work, we have incorporated ~3-nm-diameter colloidal gold (Au_c) NPs into electrospun polyethylene glycol (PEG) fibers to utilize the nanoparticle plasmonic response for localized heating and melting of the polymer to release medical treatment. Au_c and Au_c in PEG (PEG+Au_c) both exhibited a minimum reflectivity at 522 nm or approximately green wavelengths of light under ultraviolet-visible (UV-Vis) spectroscopy. PEG+Au_c ES fibers revealed a blue shift in minimum reflectivity at 504 nm. UV-Vis spectra were used to calculate the theoretical efficiency enhancement of PEG+Au_c versus PEG alone, finding an approximate increase of 10 % under broad spectrum white light interrogation, and ~14 % when illuminated with green light. Au_c enhanced polymers were ES directly onto resistance temperature detectors and interrogated with green laser light so that temperature change could be recorded. Results showed a maximum increase of 8.9 °C. To further understand how gold nanomaterials effect the complex optical properties of our materials, spectroscopic ellipsometry was used. Using spectroscopic ellipsometry and modeling with CompleteEASE® software, the complex optical constants of our materials were determined. The complex optical constant n (index of refraction) provided us with optical density properties related to

light wavelength divided by velocity, and k (extinction coefficient) was used to show the absorptive properties of the materials.

INTRODUCTION

Incorporation of metallic nanoparticles (NPs) in polymer matrix has been used for many applications. For instance, magnetic iron oxide NPs have been used as drug carriers target cancer tissue [1], gold NPs in polymer have been used to enhance light capturing of antibacterial polymers containing methylene blue [2], and silver NPs have been stabilized in polymer for antibacterial applications [3]. In addition, metallic NPs have been used for efficient heat generation [4], as localized heat sources [5], and metallic NPs linked with polymer have been used to monitor temperature change [6]. Optoelectronic applications of metallic NPs in polymer have also been investigated [7]. Gold NPs in particular exhibit a plasmonic response that can be utilized for photothermal applications [4, 8-11]. The plasmonic response of gold NPs involves electrons on the particle surface, which oscillate at resonance with incident light [11]. Non-propagating surface plasmon modes within the electromagnetic spectrum enable the conversion of optical energy to thermal energy with a concurrent temperature change within the media. It has been hypothesized that gold NPs with diameters above 2 nm have a large extinction cross-section, enabling up to 100 % light-to-heat conversion efficiency [11]. As the plasmon frequency is typically comparable with the visible light spectrum, it can be predicted that the use of plasmonic nanoparticles would enhance the photothermal conversion efficiency of materials, especially when interrogated at these wavelengths. Of particular interest, gold nanomaterials have been used to localize into cancerous tissues and cause tumor ablation due to heating upon interrogation with light [4,9,10].

In our work, we have incorporated ~3-nm-diameter colloidal gold in deionized water (Au_c) NPs into electrospun (ES) polyethylene glycol (PEG) fibers to utilize the NP plasmonic response for localized heating and melting of the polymer to release medical treatment. The Au_c used is typically sold as an all-natural and non-toxic mineral supplement that does not contain gold ions and costs $0.10/mL. In previous studies, laser mediated remote release of materials was accomplished from gold sulphide core/gold shell micro-capsules [12]. Here, we examine a topical, nanofiber mesh treatment delivery system that could be stored and used to activate drug release by illumination when needed. Ultraviolet-visible spectroscopy (UV-Vis) was used to determine the minimum reflectivity of PEG with Au_c (PEG+Au_c), PEG alone, and PEG+Au_c ES fibers. UV-Vis spectra were laid over the power spectral density curve to calculate the theoretical efficiency enhancement of PEG+Au_c versus PEG alone. Because minimum reflectivity measurements may indicate light scattered or absorbed, the light absorbed and converted to heat was determined by directly electrospinning onto resistance temperature detectors (RTDs) and converting the change in resistance to change in temperature using the Callendar-Van Dusen equation. Because PEG alone or with Au_c produces a paste-like polymer mat that would not be easily distributed as a treatment delivery material, PEG was also blended with polyethylene oxide (PEO) in order to increase viscosity and improve electrospinnability. PEG/PEO polymer blends were evaluated on differential scanning calorimetry (DSC). PEG/PEO blends containing Au_c were also tested for temperature change using RTDs. To further understand how gold nanomaterials effect the complex optical properties of our materials, spectroscopic ellipsometry was used. Using spectroscopic ellipsometry and modeling with CompleteEASE® software, the complex optical constants of our materials were determined.

EXPERIMENTAL DETAILS

Bulk Polymer and Polymer Blend Preparation

PEG or PEG+Au_c (PEG: 8,000 MW) was prepared by simple mixing on a stir plate with stir bar over 100 °C. During preparation, PEG was mixed directly into Au_c or deionized water at 58 wt%. Au_c used contained gold NPs in reagent grade deionized water and can be purchased at www.purestcolloids.com/mesogold. Au_c purchased did not contain gold ions, was sterilized prior to purchase, was stabilized with citrate, and contained an average NP diameter of 3.2 nm at a concentration of 20 ppm. Polymer blends were prepared in the same manner, with PEG and PEO (PEO: 200,000 MW) being directly mixed into Au_c. Because electrospinning requires specific polymer viscosity properties for fiber deposition, the amount of Au_c fluid was adjusted to maintain a favorable viscosity. It can be seen that this process allows some variability in the % gold in the final polymer fibers or films. Because these experiments were preliminary to show proof of concept, the amount of Au_c (deionized water plus gold colloid) was adjusted without adjusting the gold concentration in deionized water itself. In the future, altering the concentration of gold in the water prior to polymer preparation will be used to control polymer heating by Au_c at specific concentrations. See Table I for the wt% used during polymer preparation, as well as concentration (in wt%) in the final polymer fibers or film prepared:

Table I. Polymer materials ES onto resistance thermal detectors to determine temperature change.

	Material wt% During Preparation			**Concentration (wt%) in Final Polymer Fibers or Films**		
Polymer Blend (PEG: PEO)	**Polyethylene Glycol**	**Polyethylene Oxide**	**Au_c**	**% PEG**	**% PEO**	**% Gold NPs**
1:0	58.000	0.000	42.000	100	0.000	0.000
9:1	34.000	3.900	62.100	89.707	10.290	0.003
3:1	12.500	7.500	80.000	62.495	37.497	0.008
3:2	17.300	5.800	76.900	74.887	25.107	0.007
1:3	4.500	13.400	82.100	25.137	74.853	0.009

Differential Scanning Calorimetry

DSC measurements were performed in air on a TA instruments SDT-650 STA model. During the measurements, a ramp rate of 5 °C/min to 70 °C was used and followed by a 15 °C/min ramp rate up to 600 °C.

Ultraviolet-Visible Spectroscopy

UV-Vis absorption was characterized on a custom far-field probing station coupled to a spectrometer (USB4000, OceanOptics). Using the microscopy feature of the probing station, a broad spectrum light source was used to illuminate samples. Light reflected back from sample surface was collected by the microscope coupled to the spectrometer.

Energy Efficiency Calculations

Energy absorption efficiency enhancement was calculated using a trapezoidal integration of the energy absorption difference curve when considering the broad spectrum. Reflectivity (ρ) data are treated here with the assumption that $\boldsymbol{\rho} + t + \alpha = 100$ %, and $t = 0$, where t is transmissivity, and α is absorptivity. Therefore, $\alpha = 100\ \% - \rho$.

Electrospinning Parameters

In the cases of all polymer fiber creation with electrospinning, polymer delivery rate was 1.4 mL/hr, separation distance was 7.62 cm from the tip of a 20 gauge spinneret to the collection plate, and mats were spun for 5 min onto RTDs, glass slides, or a metallic collection surface. Voltage used for all polymer blends prepared in Au_c was 6.85 kV, while PEG alone in Au_c required a voltage of 7.65 kV.

Electron Microscopy

Scanning electron micrographs (SEMs) were collected on a Tescan Mira 3. Samples were gold coated for 1-2 min prior to observation and a z distance of 3-7 mm was used.

Resistance Measurements and Conversion to Temperature

Resistance measurements were taken under broad spectrum light or laser illumination on a 2450 Keithley source meter. Values were subtracted from the resistance measured from the RTD and deposited material under no light. The laser used for interrogation was green with a wavelength of 532 nm and full-scale power of 20 mW. The laser beam was contained completely on the RTD, almost completely covering the surface, and the source was held at the same distance from each sample to achieve this (10 cm). The RTD used was 2.0 mm width by 2.0 mm length, by 2.0 mm depth with a nominal resistance of 1000 Ω. Resistance measurements were converted to temperature using the Callendar-Van Dusen equation:

$$R_{ref} = [1 + A * T + B \cdot T2] \qquad \text{(Eq. 1)}$$

where R_{ref} is the reference resistance measured, A and B are Callendar Van-Dusen constants (3908×10^{-3} and 5775×10^{-7}, respectively), and T is temperature.

Thin Film Deposition and Spectroscopic Ellipsometry

Spectroscopic ellipsometry measurements were taken on polymer thin films on single side polished silicon wafer substrates. The polymers used for thin films contained the PEG/PEO (3:2) blend shown to increase to the highest temperature under laser interrogation while retaining desirable properties for distribution. Thin films were prepared by spin coating at 4000 RPM for three minutes and then running a fast cycle of 10000 RPM. Spectroscopic ellipsometry was performed on a J.A. Woollam M-2000 and the software package used for modelling was CompleteEASE®, a modelling software distributed by J.A. Woollam. During spectroscopic ellipsometry, the incident angle was set at 70° with the roughness and thickness set to fit. Film thickness was initially measured on a profilometer in order to estimate film thickness prior to performing spectroscopic ellipsometry measurements. The model in CompleteEASE® consisted of a silicon substrate layer (Herzinger *et al.*, JAP v83p3323y1998) and a B-spline set for the first layer. The B-spline layer is used to characterize partially absorbing, partially transparent films where $\boldsymbol{n}$ and $\boldsymbol{k}$ are not known prior to the measurement. The B-spline layer used contained a resolution of 0.3 eV, collected 13 points/nodes during measurement, and was set to fit optical constants and thickness.

DISCUSSION

Bulk Polymer and Electrospun Fiber Reflectivity

PEG containing Au_c was prepared at 58 wt% by adding the PEG directly to the Au_c which contained gold NPs stabilized in deionized water and letting the PEG dissolve. Once prepared, it was observed that Au_c contributed a pinkish hue to the typically clear polymer (Figure 1A). The light reddish or pink color is due to the gold NPs absorption in the lower wavelengths of light (below ~ 600 nm), and therefore reflection near the red wavelength (~ 633 nm). Bulk PEG, Au_c alone, as well as PEG+Au_c and PEG+Au_c ES fibers (Figure 1B) were placed on a reflective surface and interrogated with broad spectrum light for comparison under UV-Vis spectroscopy (Figure 1C). Results show a minimum reflectivity in both PEG+Au_c bulk polymer and Au_c at 522 nm (Figure 1D). Such a drop in reflectivity is assumed to be due to absorbed or scattered light of that particular spectrum. In our work, the purpose was to interrogate Au_c within PEG ES fibers with light to initiate electron movement on the embedded NP surface. Subsequent energy created in the form of heat would be used to melt the fibers and deliver medical dopants. When PEG+Au_c ES fibers were interrogated with light, minimum reflectivity was slightly blue shifted to 504 nm (Figure 1D). In either case, minimum reflectivity occurred in green wavelengths of light which range from 500-565 nm.

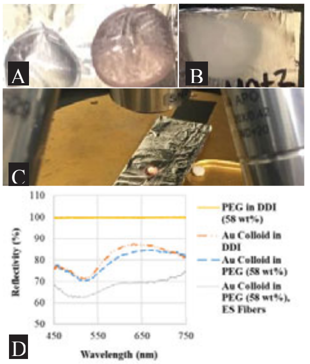

Figure 1. A Bulk polymer samples showing PEG dissolved in deionized water (58 wt%) and PEG dissolved in Au_c (58 wt%). **B** PEG+Au_c polymer after being ES into a mat. **C** PEG+Au_c bulk polymer under far field probing station used to collect UV-Vis spectra. **D** Under broad spectrum white light illumination, maximum reflectivity of Au_c or Au_c in PEG can be seen at 522 nm. When ES into fibers, PEG+Au_c has a blue shifted maximum reflectivity at 504 nm, and the response is slightly mitigated as compared to Au_c or PEG+Au_c.

Energy Efficiency Calculations

Reflectivity measurements were used to calculate the energy absorption for gold colloid/PEG interrogated with white and green light (Figure 2). Energy absorption for PEG+Au_c showed a maximum energy absorption efficiency enhancement of ~14 %. The intensity spectrum is shown for a tungsten lamp filtered in the green and a continuous-wave green laser source. Efficiency enhancement across the 450 to 750 nm spectrum was calculated to be ~10 % using trapezoidal integration. The energy enhancement is significant in that a system that is 14 % more efficient in converting optical energy into thermal energy would allow a system that can be 14 % more efficient in its power source or can last 14 % longer between recharge. Further enhancement is desired, and can be achieved with further increase in the optical-to-thermal plasmonic energy conversion mechanism.

Electrospun Fiber Morphologies

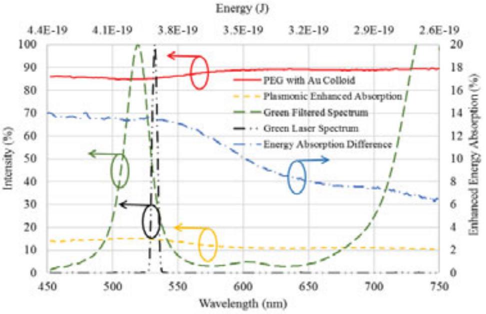

Figure 2. Reflectivity measurements were used to calculate the theoretical energy absorption for PEG+Au$_c$ interrogated with white and green light. Calculations showed a peak energy efficiency of ~14 %. The green filtered spectrum and green laser spectrum overlap the energy absorption difference curve just below the 14 % level.

Electrospinning of PEG+Au$_c$ resulted in electrospraying and created a mat with a paste-like texture that could not be peeled up easily from the deposition surface (Figure 3A). In order to induce characteristics conducive to a treatment delivery system that could be stored and distributed, PEO was blended into the PEG+Au$_c$ mix to enhance viscosity and improve the final material properties. DSC measurements showed that the mixing of PEO and PEG created a true blend as expected, in which the melting temperature of the blended polymers corresponded to the higher melting point of two polymers. Results from DSC are listed in Table II.

Table II. PEG/PEO polymer blend used for desirable material properties of the ES mats.

Sample Type	Molecular Weight	Melting Point (°C)
PEG	8,000	63
PEO	200,000	71
PEG/PEO	60:40 wt% Respectively	71

Incorporation of PEO did provide ES fiber mats with desirable characteristics for distribution and could be peeled from the deposition surface as one material easily. However, because polymer chain length increases melting temperature [13] incorporation of PEO had to be minimal so as to not increase the intensity of light interrogation required to melt the ES fibers. To determine the minimum amount of PEO that resulted in fiber mats with desirable characteristics, several polymer blends containing Au$_c$ were prepared and ES. Polymer blends prepared were the following: 1) 3:1 PEG to PEO (Figure 3B), and 2) 9:1 PEG to PEO (Figure 3C), 3) 1:3 PEG to PEO (Figure 4A), 4) 1:1 PEG to PEO (Figure 4B), 5) 3:2 PEG to PEO (Figure 4C). SEMs revealed that in all cases, ES fiber diameters ranged from 800-1,000 nm (Figure 3-4). While in all cases, fibers did have weak areas where the fiber was pinched, increased PEG led to a greater number of these weak areas pinched to a greater extent (Figure 3C). While the 3:1 and 9:1 PEG to PEO polymer blends still resulted in paste-like materials being deposited (Figure 3), 1:3, 1:1, and 3:2 PEG to PEO polymer blends resulted in peelable mats which could be distributed (Figure 4).

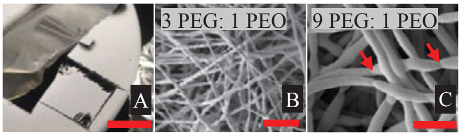

Figure 3. A The fiber blends shown were ES onto RTDs so that change in resistance under light illumination could be measured. When PEG-only was ES, the deposited material was paste-like. (Scale = 1cm) **B-C** SEMs showing PEG/PEO polymer blend ES into fibers. Increased PEG in the fibers resulted in weaker fibers which were pulled apart at various locations throughout the fibers (examples indicated by arrows). (Scale = 5 µm)

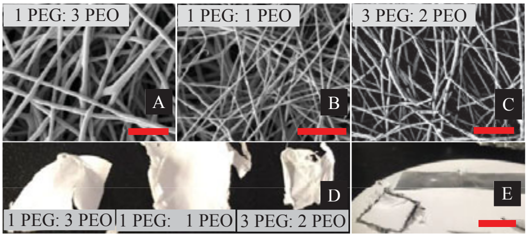

Figure 4. A-C SEMs showing PEG/PEO polymer blends prepared at various wt% and ES into fibers (Scale = 5µm). **D** Polymer blends shown in **A-C** created fiber mats which could be peeled from the deposition surface for distribution. **E** Photograph of the deposition plate used to deposit ES fibers directly onto RTD's so that resistance under light illumination could be measured. (Scale = 1 cm)

Light Induced Temperature Change in Bulk Polymers and Electrospun Fibers

As shown in Figures 3C and 4E, PEG+Au$_c$ or PEG/PEO+Au$_c$ composite polymer blends were ES directly onto RTDs so that resistance under light interrogation could be measured and converted to temperature change using the Callendar-Van Dusen equation. To maximize the effect, a green laser was used to illuminate the RTD surface directly. Fiber mats made from PEG+Au$_c$ without PEO increased in temperature the maximum at 9.0 °C (Figure 5). ES fibers made from the 9:1 PEG to PEO mix were just under the maximum, increasing fiber mat temperature to 8.9 °C (Figure 5). However, as stated in the previous section, the 9:1 PEG to PEO mix did not produce a fiber mat with distributable properties. The second and third highest temperature increase occurred in the 3:2 and 3:1 PEG to PEO polymer mixes, increasing fiber mat temperatures by 6.8 °C and 7.4 °C, respectively (Figure 5). In the previous section, it was discussed that the 3:2 PEG to PEO fiber mix did produce a peelable fiber mat which could be distributed for use as a drug delivery system, and therefore represented the desirable PEG/PEO+Au$_c$ polymer blend which should be used for light-induced drug delivery fibers. Most promising is the little amount of gold that is needed to cause the observed temperature changes. In the desirable polymer blend described (3:2 PEG to PEO), the gold concentration used was only 0.007 % (Table I). That coupled with the inexpensive Au$_c$ purchased for this work ($0.10/mL) make a plasmonic responsive drug delivery bandage a feasible medical treatment delivery system.

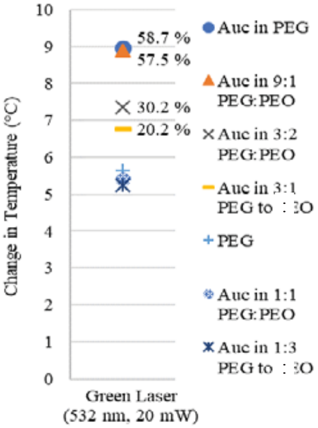

Figure 5. PEG, PEG/PEO polymer blends, and PEG/PEO polymer blends containing gold NPs were ES directly onto RTD's. Change in resistance of RTD's under illumination by green laser light was measured and converted to temperature. Polymer blends containing 50 % or more PEO did not elicit an increase in temperature under illumination. Of the polymer blends that did increase in temperature, the gold NP-containing 3:2 PEG to PEO blend increased temperature by 7.4 °C while providing the appropriate material properties for distribution. Comparatively, this increase is 30.2 % when compared to PEG-only fibers. Percentages indicate temperature enhancement as compared to PEG only fibers.

Complex Optical Properties of Gold Doped Polymer

Spectroscopic ellipsometry measurements were used to determine the difference in complex optical properties of polymer thin films containing only PEG/PEO

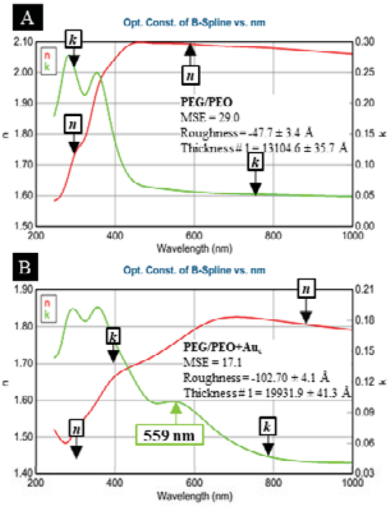

Figure 6. Spectroscopic ellipsometry data collected and modeled in CompleteEASE® software. **A** Complex optical constants of 3:2 PEG to PEO polymer blend film. Results show a drop in absorption approaching a minimum after approximately 400 nm. The drop in absorption is reflected by the refractive index of the material, indicating an increase in optical density beyond this wavelength as well. **B** Complex optical constants of the same polymer blend in **A** but containing gold NPs. From this data, a unique absorption peak can be seen at 559 nm, indicating the gold NPs enhanced absorption of the polymer film at this wavelength. This unique peak is reflected by a very minimal dip in the refractive index, indicating that the material exhibits a drop in refraction at this point as well.

versus PEG/PEO+Au$_c$. Results revealed an obvious change in the complex optical properties of the films when Au$_c$ was doped into the polymer (Figure 6). For the PEG/PEO only film, absorption (***k***) continued to approach a minimum after a wavelength of 400 nm, whereas the PEG/PEO+Au$_c$ film demonstrates a unique peak in absorption at a wavelength of 559 nm. This peak shows that the Au$_c$ in the thin film creates enhanced absorption of the polymer blend at this green wavelength of light. Mean square error (MSE) for the films were 29.0 for the PEG/PEO film, and 17.1 for the PEG/PEO+Au$_c$. Although these values appear high, the CompleteEASE® software manual indicates that while an MSE of ~1.0 is achieved for single thin films on Si substrates, thickness and multiple layers present complex modelling that and may exhibit MSE's >10.0 and still be considered acceptable. In the future, modification of deposition substrates and matching of thermal expansion properties of materials will be used to minimize these values further.

CONCLUSIONS

In the work presented, gold NPs were embedded in polymer fiber meshes using electrospinning. Because gold NPs exhibit a plasmonic response when interrogated with light, it was anticipated that polymer embedded with gold NPs could be externally interrogated with light, initiating a plasmonic response that resulted in localized energy in the form of heat at the gold NP surface. Generated heat could then melt the surrounding polymer embedded with medical treatment for an on-demand treatment delivery system.

Prepared polymers of PEG 58 wt% and PEG+Au$_c$ (58 wt%) were characterized under UV-Vis spectroscopy, finding a minimum reflectivity at 522 nm in both sample types. The data collected were used to calculate theoretical energy absorption of the materials. Energy absorption efficiency enhancement of the PEG+Au$_c$ versus PEG alone was calculated using a trapezoidal integration of the energy absorption difference curve. The near 14 % enhancement of photon to thermal energy conversion may translate into a drug delivery system that is 14 % smaller or has a 14 % longer lifetime, both desirable results for efficient on-demand drug delivery.

Also in these investigations, the reflectivity of PEG+Au$_c$ ES fibers under broad spectrum light was characterized through UV-Vis spectroscopy as having a minimum reflectivity at 504 nm, corresponding to green wavelengths of light. However, PEG+Au$_c$ formed a paste-like substance that could not be peeled up from a deposition surface and broadly distributed as a drug delivery material. Therefore, PEO was incorporated into PEG+Au$_c$ in order to add viscosity to the prepared polymer for electrospinning so that a distributable fiber drug delivery system could be fabricated. Because PEO has a longer polymer chain length than PEG, it too has a correspondingly increased melting temperature which would require greater light interrogation for melting. To mitigate the amount of PEO used without sacrificing desirable material properties, several PEG/PEO+Au$_c$ blends were ES into fiber mats. Results showed that a blend of 3:2 PEG to PEO resulted in a "peelable," and therefore distributable fiber mat. Further investigations required directly electrospinning all Au$_c$ fiber blends directly onto RTDs so that temperature change could be measured. In those studies, it was found that PEG+Au$_c$ experienced the greatest temperature increase (9.0 °C) when interrogated with green laser light. As expected, incorporation of PEO decreased the temperature change experienced by the polymer fibers. However, when a mix of 3:2 PEG to PEO was tested, an increase of 7.4 °C was recorded, while still maintaining a fiber mat that could be peeled from the deposition surface for distribution. Such results indicate this particular blend may be most ideal for creating a distributable, on-demand drug delivery system with desirable material properties. Most promising is the little amount of gold that is needed to cause the observed temperature changes. In the desired polymer blend described (3:2 PEG to PEO), the gold concentration used was only 0.007 % (Table I). That coupled with the inexpensive Au$_c$ purchased for this work ($0.10/mL) make a plasmonic responsive drug delivery fiber mesh a feasible medical treatment delivery system.

Finally, the complex optical constants of the nanogold doped polymers was determined using spectroscopic ellipsometry. Spectroscopic ellipsometry measurements and model development showed an obvious change in the complex optical properties of the films when Au$_c$ was doped into the polymer. For the PEG/PEO only film, absorption ($\boldsymbol{k}$) continued to approach a minimum after a wavelength of 400 nm, whereas the PEG/PEO+Au$_c$ film demonstrates a unique peak in absorption at a wavelength of 559 nm. This peak shows that the Au$_c$ in the thin film creates an enhanced absorption of the polymer blend at this green wavelength of light. Such models will be used in the future to determine desirable optical properties of our materials.

ACKNOWLEDGMENTS

The authors would like to thank James Hilfiker, engineer at J.A. Woollam, for his consulting efforts on our spectroscopic ellipsometer models. The research presented has been funded by two entities: (1) Army Research Laboratory (cooperative agreement) and (2) the National Science Foundation (Established Program to Stimulate Competitive Research or EPSCoR).

Research was sponsored by the Army Research Laboratory and was accomplished under Cooperative Agreement Number W911NF-15-2-0020. The views and conclusions contained in this document are those of the authors and should not be interpreted as representing the official policies, either expressed or implied, of the Army Research Laboratory or the U.S. Government.

The U.S. Government is authorized to reproduce and distribute reprints for Government purposes notwithstanding any copyright notation herein. This material is based upon work supported by the National Science Foundation under Grant No. OIA-1757351. Any opinions, findings and conclusions or recommendations expressed in this material are those of the author(s) and do not necessarily reflect the views of the National Science Foundation."

References:

[1] K. Ulbrich, K. Holá, V. Šubr, A. Badandritsos, J. Tuček, and R. Zbořil, Chem. Rev. 116, 5228-5431 (2016).

[2] S. Perni, C. Piccirillo, J. Pratten, P. Prokopovich, W. Chrzanowski, I. P. Parkin, and M. Wilson, Biomaterials 30, 89-93 (2009).

[3] D. Maity, AmK. Bain, B. Bhowmick, J. Sarker, S. Saha, K. Acharya, M. Chakraborty, and D. Chattopadhyay, J. Appl. Polym. Sci. 122 (4), (2011).

[4] A.O. Govorov and H.H. Richardson, Nano Today 2, 30-38 (2007).

[5] S. Maity, L. N. Downen, J. R. Bochinski, and L. I. Clarke, Polymer 52, 1674-1685 (2011).

[6] J. Lee, A.O. Govorov, and N.A. Kotov, Laser Surg. Med. 37 (2), 123-129 (2005).

[7] S. Li, M.M. Lin, M.S. Toprak, D.K. Kim, and M. Muhammed, Nano Rev. 1, (2010).

[8] K. Jiang, D.A. Smith, and A. Pinchuk, J. Phys. Chem. 117 (51), 27073-27080 (2013).

[9] C. Bi, J. Chen, Y. Chen, Y. Song, A. Li, S. Li, Z. Mao, C. Gao, D. Wang, H. Möhwald, and H. Xia, Chem. Mater. 30 (8), 2709-2718 (2018).

[10] X. Huang, I.H. El-Sayed, W. Quian, and M.A. El-Sayed, J. Am. Chem. Soc. 128 (6), 2115-2120 (2006).

[11] V. Amendola1, R. Pilot, M. Frasconi1, O. M. Maragò, and M. A. Iatì, J. Phys.-Condens. Mat 29 (20), (2017).

[12] A.G. Skirtach, C. Dejugnat, D. Baaun, A.S. Susha, A.L. Rogach, W.J. Parak, H. Mϕhwald, and G.B. Sukhorukov, Nano Lett. 5 (7), (2005).

[13] M. Rubinstein and R. H. Colby, Polymer Physics, edited by Oxford University Press (Oxford, New York, 2003), p. 5.